Range-based techniques for discovering optimality and analyzing scaling relationships in neuromechanical systems.

Bradly Alicea
MIND Lab, Michigan State University

Keywords: scaling laws, neuromuscular systems, neuromechanics, analytical techniques

Abstract. In this paper, a method for decoupling the neuromuscular function of a set of limbs from the role morphology plays in regulating the performance of an activity is introduced. This method is based on two previous methods: the rescaled range analysis specific to time series data, and the use of scaling laws. A review of the literature suggests that limb geometry can either facilitate or constrain performance as measured experimentally. Whether limb geometry is facilitatory or acts as a constraint depends on the size differential between arm morphology and the underlying muscle. "Changes in size and shape" are theoretically extrapolations of morphological geometry to other members of a population or species, to other species, or to technological manipulations of an individual via prosthetic devices. Three datasets are analyzed using the range-based method and a Monte-Carlo simulation, and are used to test the various ways of executing this analysis. It was found that when performance is kept stable but limb size and shape is scaled by a factor of .25, the greatest gain in performance results. It was also found that introducing force-based perturbations results in 'shifts' in the body geometry/performance relationship. While results such as this could be interpreted as a statistical artifact, the non-linear rise within a measurement class and linear decrease between measurement classes suggests an effect of scale in the optimality of this relationship. Overall, range-based techniques allow for the simulation and modeling of myriad changes in phenotype that result from biological and technological manipulation.

Introduction

Neuromechanical systems are adaptive entities that involve interplay between adaptation, the automation of behavior by the nervous system, and the constraints of limb geometry (Enoka, 2002). One such factor in determining performance involves differences in intralimb proportions for a specific morphological system. Intralimb proportions are also physically variable in a way that is predictable across individuals and populations (Holmes et.al, 2006). This is a product of evolutionary forces. Trait size is controlled by the rate of cell proliferation both locally and globally in the phenotype (Emlen and Allen, 2004). Another factor that determines performance is adaptation based on the interaction of neuromuscular behavior and adaptation. There are various regularities in the properties of muscle mass, muscle fiber composition, and mechanical advantage during function that is related in a linear fashion when compared across phenotypes of different sizes (Barry and Enoka, 2007; Rome, 1999).

In this paper, a method that elucidates relationships between limb geometry, neuromuscular output, and variation in form will be introduced and applied to three datasets. In the first dataset, the range of both performance indicators and phenotypic measurements are rescaled into four different transformation classes. In the second dataset, which focuses on exploration of tactile surfaces, performance indicators and phenotypic measurements are simulated using a Monte Carlo approach. The third dataset is derived from an experiment similar to the first, and replicates the analysis done on the first experiment.

Theoretical Reasoning. There are three theoretical reasons why morphological geometry is thought to be related to performance measurements. The first reason involves a principle called constructal theory (Bejan, 2000), which predicts that biological structures evolve to maximize the flow of energy and productive output. In the case of animal limbs and neuromuscular systems, it has been found that

muscular output and limb size are linearly related (or allometric), and that this relationship is specific modes of locomotion (Bejan and Marden, 2006).

The second reason why morphological geomentry is an important factor in performance has to do with different predictions regarding the stability of a limb during movement. Gomi and Kawato (1996) proposed the equilibrium-point hypothesis, which predicts that an invisible center of stability exists along the axis of the arm or leg during the course of a movement. Efficiency and mechanical advantage is maximized when this invisible point is closest to the actual joint. Put in terms of movement space around the individual, areas reachable by the limb during movement form a manifold, which extends the axis of movement to provide a maximal degree of stability and mechanical advantage (Scholz and Schoner, 1999).

The third reason why morphological geometry is an important factor in performance takes into account the first two and involves artificially manipulating both geometric parameters of the arm segments and output of the neuromuscular system. This is done to better understand how prosthetic devices in addition to changes of geometry in development and aging and differences across individuals influence the stability and efficiency of the morphology. In natural systems that exhibit proportional function between size or shape and output, decreases in one variable are linearly offset by the increases in the other in a manner previously referred to as scale invariance (Brown et.al, 1999; Brown et.al, 1997). The extent of this efficiency is expressed by a relationship between scaling manipulations between these variables (Bejan and Marden, 2006). Taken collectively, this result describes the effects of the simulated environment on the control of muscular output and the morphological geometry by varying both of these independently and systematically.

Examples of relationships between morphological geometry and performance. One mechanism that acts as a physiological limit to human performance is the allometric scaling of phenotypic traits (Cheverud, 1982). In adult organisms, scaling of the limbs generally minimizes the energetic requirements for movement (Full and Koditschek, 1999). For example, the ratio of shank length to thigh length can be optimized at a value of 1.06 relative to stability and energetic efficiency in stripped-down physical models of gait (Collins et.al, 2005). The functional morphology of upper-body limbs is also expected to yield an optimal state among specific scaling ratios as has been demonstrated in the design of biologically-inspired robots (Hara and Pfeifer, 2003, Page 59). Such differences are also expected to yield optimal performance for certain scaling values. As this mechanism is related to growth regulation in development, it is independent of behavioral adaptations forced by perturbed environments. In terms of standing variation, there is a role for morphological dampening (Full and Koditschek, 1999). Morphological dampening occurs when body morphology enforces a physical constraint upon the plastic response of physiological systems.

Methodology

The range-based method is based in part on the rescaled range analysis (Hurst, 1951), which is used in time-series to find patterns that might repeat at different points in the future. In this case, I am interested in order of magnitude effects on variation in morphology and performance rather than temporal effects, so the method was modified to exclude calculation of a Hurst exponent. It is predicted that fitness increases for a greater number of morphologies at the upper (e.g. larger) end of the distribution. This information can be extrapolated to a potentially extreme range of variation or the design of wearable devices that augment the size and shape of the arm.

In this paper, the concept of morphological scaling will be used to discover the complexity of

physiological systems involved with neuromechanical-related performance and adaptation. Scaling laws have been used in a number of contexts to explain physiological phenomena, from the functional outcomes of growth and form (Huxley, 1932) to the structure of metabolic rates and vasculature across species (West et.al, 1997). In this context, the following question can be asked: what does an indicator of movement activity look like when morphology is scaled by factors of .25 or vice versa? West et.al (2005) discovered a ¼ power law scaling relationship that is widespread in biological systems, and appears to be a fundamental principle of biological self-organization. Not only is ¼ power law scaling ubiquitous in natural systems, but scale invariance across systems based on the intersection of opposing trends in the same system is also common.

Four analytical techniques are introduced in this paper. The first is the range-reduction method for hypo- and hyper-allometry. In this approach, the range of each measurement is characterized in terms of relative variance. An extremely hyper-allometric relationship means that performance variation is maximized during the treatment condition. An extremely hypo-allometric relationship means that performance variation is minimized during the treatment condition. The second approach is the range-reduction method itself. In this case, the range for both measurements are reduced by either two or four factors (e.g. 0.25, 0.50, 0.75, 1.0) relative to a performance indicator. The goal is to find what combination of reduction factors result in increases or decreases of the performance indicator. The third technique involves a Monte Carlo simulation that extrapolates experimental results to a population of thousands. The effects of morphological variation on performance differ for different portions of the performance/limb geometry function given different surface conditions and cumulative effects (see Notes on experimental procedures). The fourth technique used for is an optimal point analysis, which involves using a frequency analysis to find the median of the performance and limb geometry distributions. The median for both distributions is then treated as a point on a two-dimensional space. Limb geometry measurements were derived from the human standing height, forearm, and humerus, while the muscle measurements were derived from the triceps brachii (TB - humeral muscle) and flexor carpi radialis (FCR - forearm muscle)[1].

Purpose of the range-based method. The purpose of this test is to detect violations of expected scale invariance. The null hypothesis is that the proportion of limb size (in this case the proportion of limbs in the anatomical system at work) scales at a factor of n, while the movement performance indicator scales at a factor of –n. This suggests the bounds of adaptability, represented by the size and shape of the adult phenotype, has an implicit effect upon performance level expressed as a set of relationships with complex aspects of phenotype geometry. In the case of the null hypothesis, while one variable exhibits positive allometry (or function with a positive slope), the other variable exhibits a nearly identical degree of negative allometry (or function with a negative slope). Based on this observation, a prediction can be made: scaling the range of each of these variables by progressive factors of .25 should yield a stable measurement for all possible values[2]. Any increase in the performance measurement for any transformation of these categories is an indicator of an optimal configuration of the limbs involved in the experimental activity. This can also be demonstrated by an increase or decrease in the slope of the limb proportion/performance measurement relationship. In this case, a transformation of the phenotype is said to have a hyper- (increase) or hypo- (decrease) allometric effect on this relationship.

General Approach. The range of both morphological and performance measurements were scaled by a

[1] Consult the Methods and Measurements section for more details.

[2] All possible values are defined for limb proportions, movement performance measurement are as follows: .25, 1.0; 1.0, .25; .50, 1.0; 1.0, .50; .75, 1.0; 1.0, .75; and 1.0, 1.0. A value of 1.0 is considered to be a control condition.

series of factors in combinatorial fashion to identify performance as a function of body size. This was done to uncover a complex relationship between the allometric scaling and the performance measurement which can be explained in terms of scale invariance. When the geometry and output of the system is maximally efficient, a linear relationship between scaling classes should be expected. If not, either a simple or complex curvilinear relationship should exist.

Transformation of the phenotype. Figure 1 demonstrates the effect of scaling transformations on a human forelimb with the muscles represented by passive springs. The scaling transformation is conducted on an "averaged idealized organism", which simply means that it is not representative of any particular individual. In the upper left frame, a morphology that has a humeral-to-forearm ratio of .971 is scaled by a factor of .25. This results in two different but equivocal transformations: either a humerus that is 25% of its original size, or a forearm that is 25% of its original size. The assumption made in this method is that the mechanical advantage of the arm is constant across a specific activity, characterized by measurements of performance.

Data Interpretation: Range Reduction method for hypo- and hyper-allometry.

To better understand the magnitude of effects between arm morphology, physiology, and behavior, I conducted a set of computational experiments on the data. These experiments were motivated by an observation that the range of each variable contributed to the shape of the function. In addition, there were concerns regarding whether specific blocks produced hyper- or hypo-allometric effects.

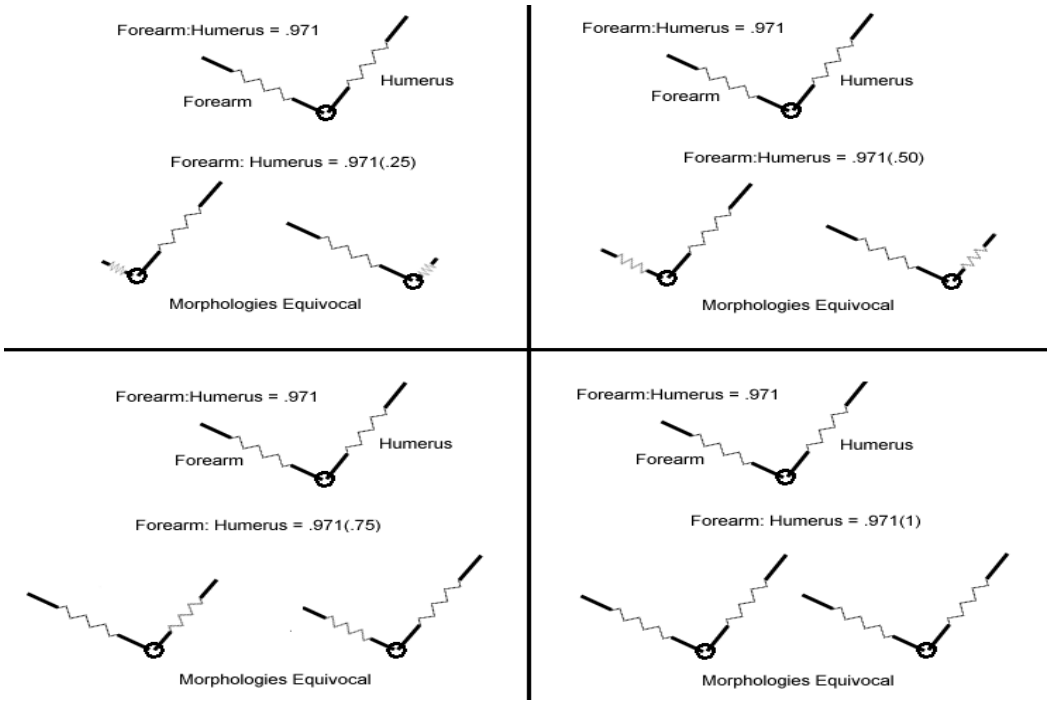

Figure 1. An example of rescaled morphologies using a biomechanical model of the human arm.

The size and shape of the humerus and forearm were computed using several measurements[3]. Each approximation of volume was then scaled against each other. The regression equation and scaling

[3] The size scaling was calculated by comparing the volume of two cylinders: one representing the forearm, and the other representing the humerus. Volume was the product of the circumference and length of each segment. The shape scaling was calculated by dividing the height (in this case the diameter of the segment) by the width for both segments. For symmetrical shapes such as a square, this results in a value of 1.

factors (i.e. b_1 and b_2) were calculated for these relationships, in addition to a range-based normalization of the function shape. Results of this analysis are shown in Table 1. The features of the upper left frame in Figure 1 hold true for all of the other examples. Scaling the forelimb by a factor of 1.0 (or 100%) serves as a virtual control.

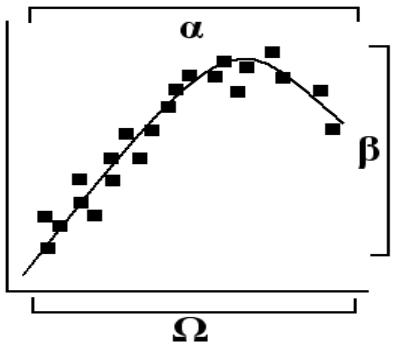

Figure 2. Schematic of range-based calculation for hypo- and hyper-allometry. Three parameters for derivation of calculation: α is the range along the x-axis (scaling), β is the range along the y-axis (performance measurement), and Ω is the artificial scaling of the data by some factor. NOTE: the parameter Ω can refer to the x-axis, the y-axis, or both. Shown here is the parameter Ω with a value of 1.0 for the x-axis.

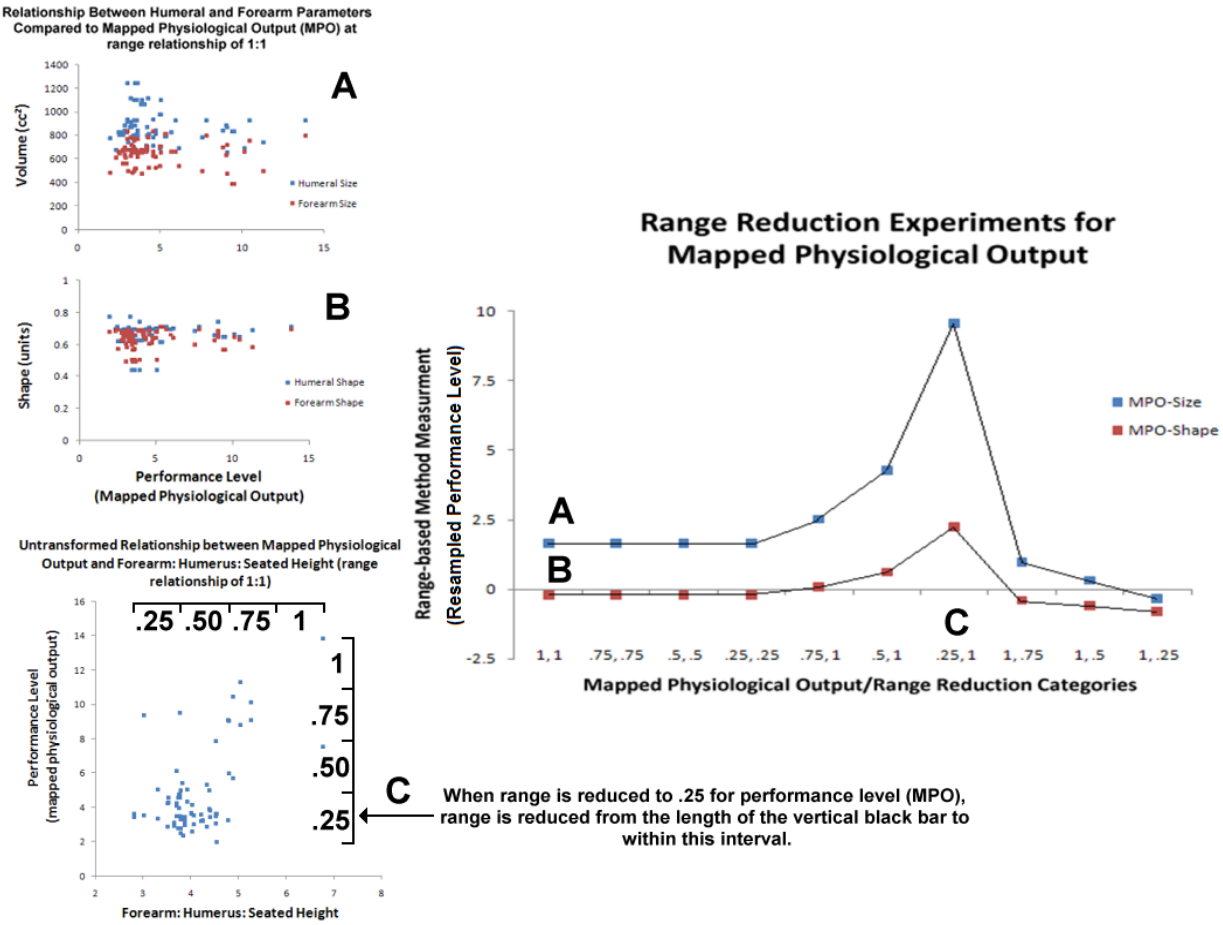

Figure 3. Results for range reduction experiments conducted on mapped physiological output data (range-based measurement averaged across experimental blocks). Main graph is displayed on right-hand side. Reduction categories are listed as *m,n*, where *m* is reduction/enlargement of performance measure, and n is reduction/enlargement of the allometric scaling. A and B represent the normal range of size and shape vs. performance level before range reduction. C is the relationship between performance scaling and performance level before range reduction.

Specifics of range reduction method. To test the robustness of these specific performance-morphology relationships, a range of potential performance and anatomical resamplings were conducted[4]. For the mapped physiological output measurement, the following question was asked: if the range of phenotypes or performance responses to perturbations of greater magnitudes are expanded or reduced, what would the effect be on the regression equation? In simpler terms, changes in magnitude for either of these factors were expected to enhance the degree of hyper- or hypo-allometry in this scaling relationship.

Range-reduction calculation of hyper- and hypo-allometry. To normalize the effects of reducing the range of one or both axes, a measurement was used to capture the shape of the nonlinear regression function[5]. When the value of this measurement is 0, it is roughly equivalent to a monotonic linear function. Positive values indicate an increase in the range of the y-axis relative to the x-axis (hyper-allometry), while negative values indicate an increase in the range of the x-axis relative to the y-axis (hypo-allometry). To achieve this, three parameters are defined: α, β, and Ω. Alpha is the range of data on the x-axis (which is the maximum value subtracted by the minimum value), beta is the range of data on the y-axis, and omega is the reduction of the range of data on either or both axes by some factor. The schematic in Figure 2 describes these relationships in graphical form. This increase or decrease in the allometric relationship is relative to a slope of 1.0, which represents a standard allometric relationship where both variables contribute equally to the variance.

Figures 3 and 4 demonstrate the range-based method measurement value for a range of scaling and performance measurement reductions. In both figures, mapped physiological output and the size (blue) and shape (red) scalings were reduced by 25 (.25), 50 (.5), and 75 (.75) percent. The values on both axes were also held constant (at a value of 1.0). These manipulations demonstrate how changes in each variable may affect interactivity in a number of potential settings. For example, reducing the performance measurement while keeping the morphological scaling constant results in a large increase in the range-based measurement, and indicates significant hyper-allometry. When the opposite manipulation is performed (reducing the morphological scaling while keeping the performance measurement constant), the range-based measurement tends towards hypo-allometry.

Figure 4 shows the same set of experiments conducted on the muscle measurements. Triceps brachii (TB) activity, flexor carpi radialis (FCR) activity, and the size (blue) and shape (red) scalings were reduced by 50 (.5) percent. As in the case of mapped physiological output, the values on both axes were also held constant (1). As in the case of mapped physiological output, reducing the performance measurement by 50 percent (0.50) increases the range-based measurement by a similar magnitude for both muscles. Also similar to what is observed with the mapped physiological output performance measurement, the size scaling shows a larger effect than the shape scaling.

In this instance, the size transformation of the limb geometry data is inherently hyper-allometric, while the shape transformation is inherently hypo-allometric. Nevertheless, there are apparent shifts within the experiment and change with switching between perturbation and normal treatment conditions. The results of this technique were inconclusive, but trend towards either recovery in the

[4] The purpose of the range-based method is to assess hypothetical growth and form scenarios in development and evolution. While done in an abstract manner, the range-based method identifies potential constraints that could affect behavioral fitness as measured using the metric shown in equation [8].

[5] The range-based calculation is RBC = [(α) * (Ω_x)] / (β) * (Ω_y)] – 1. When the range of both the x- and y-axes are equal, is results in a value of 1. Subtracting 1 from this value results in 0, which represents a "neutral" nonlinear function.

third block to the first or change in the third block as compared with the first and second. This is consistent with how the performance measurements change as plotted alone over the same set of experimental blocks and perturbations (see Alicea, 2008).

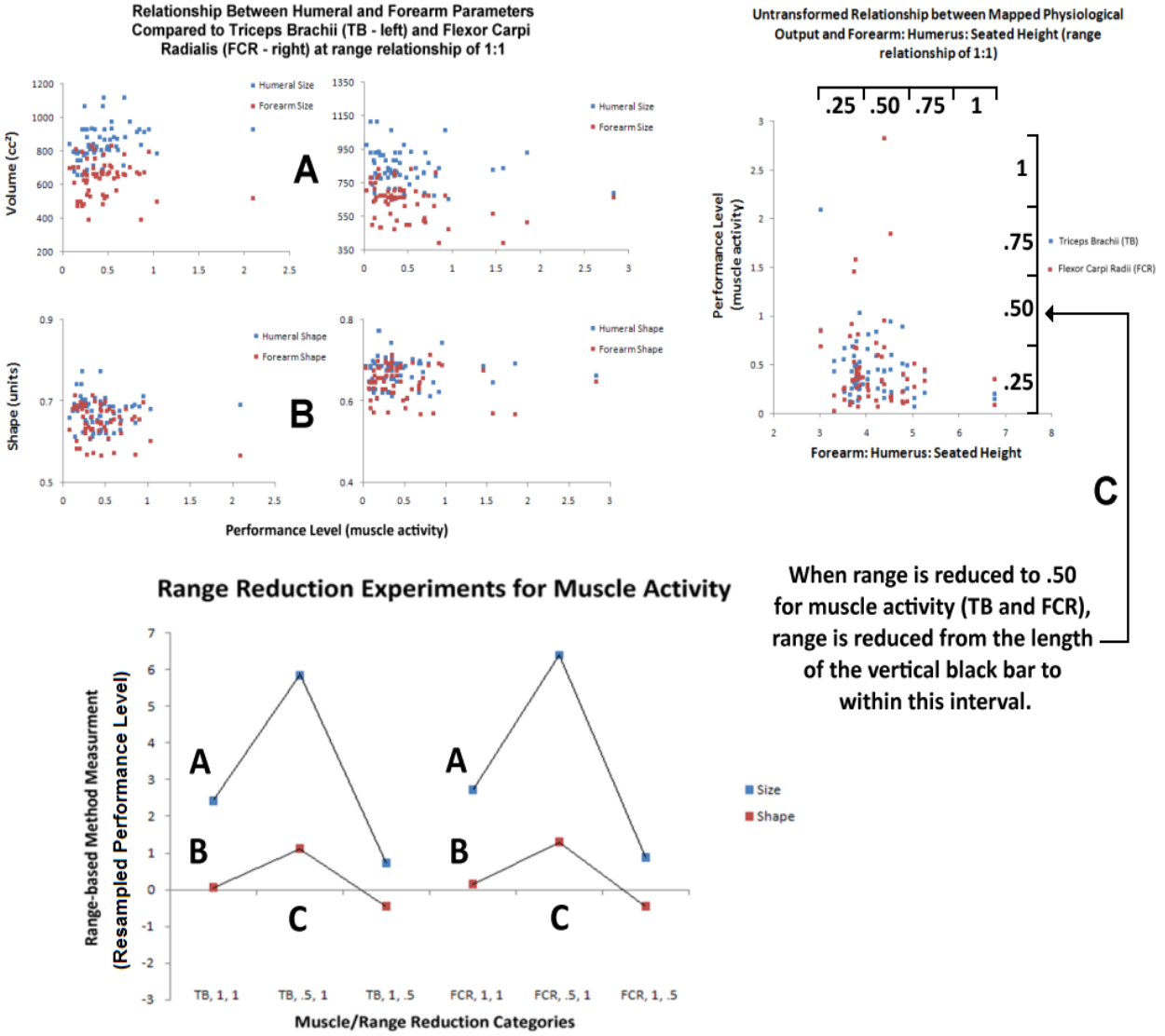

Figure 4. Results for range reduction experiments conducted on muscle activity data. TB = triceps brachii, FCR = flexor carpi radialis (range-based measurement averaged across experimental blocks). Main graph is displayed at bottom. Reduction categories are listed as *m,n*, where *m* is reduction/enlargement of performance measure, and n is reduction/enlargement of the allometric scaling. A and B represent the normal range of size and shape vs. performance level before range reduction. C is the relationship between performance scaling and performance level before range reduction.

The far right column in Table 1 provides a range of values that determine how much morphological proportions and performance measures vary when the transformations are not applied. The greatest degree of hyper-allometry is exhibited when the muscle activity of triceps brachii and flexor carpi radialis is scaled against the humerus-to-forearm size measurement. In Figures 3, 4, 7, and 8, a factor between .25 and 1 were used for both variables. For mapped physiological output, the greatest effect of hyper-allometry is when performance is reduced by a factor of .25 and the allometric scaling is not reduced. For both muscles, the greatest effect is when the performance measure is reduced by a factor of .50 and the allometic scaling is not reduced. This true for both size and shape measurements. This

speaks to how adaptable the physiological mechanisms are under the experimental conditions, especially when the size and shape of the phenotype are held constant.

Table 1. Statistics related to performance scaling regression by approximation of arm anatomy, experimental block, and performance measurement.

Criterion	Measure	Block	Regression Coefficient	b_1	b_2	Hypo/Hyper-allometry (range-based method) *
Size	MPO	1	0.165	4.583	-8.243	1.65
Size	MPO	2	0.374	2.179	-5.204	1.55
Size	MPO	3	0.197	4.424	5.127	1.73
Shape	MPO	1	0.041	0.975	-1.65	-0.18
Shape	MPO	2	0.1	0.209	-0.617	-0.22
Shape	MPO	3	0.083	0.875	-1.612	-0.16
Size	TB	1	0.102	-14.05	6.147	2.87
Size	TB	2	0.099	4.487	-2.95	1.66
Size	TB	3	0.045	6.097	-3.175	2.69
Shape	TB	1	0.054	-3.152	1.355	0.19
Shape	TB	2	0.037	0.863	-0.563	-0.18
Shape	TB	3	0.167	4.222	-2.069	0.14
Size	FCR	1	0.096	12.12	-5.537	2.91
Size	FCR	2	0.064	2.177	-1.764	3.07
Size	FCR	3	0.124	5.187	3.589	2.13
Shape	FCR	1	0.097	3.772	-1.737	0.20
Shape	FCR	2	0.135	0.975	-0.791	0.25
Shape	FCR	3	0.145	1.905	-1.276	-0.03

*** value for Ω in hypo/hyper-allometry calculation held constant at 1 across all comparisons.**

In Figure 4, there is a spike when the performance measure is scaled by a factor of .75, .50, and .25 and the morphology is left at 1.0. In Figure 5, there is a spike when the performance measure is scaled by a factor of .50 and the morphology is left at 1.0. In both cases, it appears that when the range of the performance measure is reduced and the range of the morphological data is held constant at 1.0, there is an overall increase in the performance measure. This suggests a degree of hyper-allometry in the comparison between performance and morphology: performance improves faster than traits get larger. This result also suggests that hyper-allometry in the performance allometry function is a signature of increases in relative fitness for certain parts of the sampling population.

Figures 3, 4, 7, and 8 are divided up into three parts. The two insets on each graph show the raw data and their distributions. The larger graph entitled "range reduction experiments" shows the final result of this method. On the y-axis is the range-based method measurement, which is the performance data for each muscle and mapped physiological output. The x-axis has a combinatoric series of data resamplings for both selected morphological and performance measurements. For example, .50, 1.0 corresponds to a performance measure with half the range of the original dataset and a morphological measurement representing the total range of the original dataset. Reference to this is made in the inset label C on both graphs. Two morphological measurements are used in comparison, but result in the same function. The blue function represents a size calculation of the arm segments, while the red function represents a shape calculation of the arm segments (the dominant arm for each individual was used).

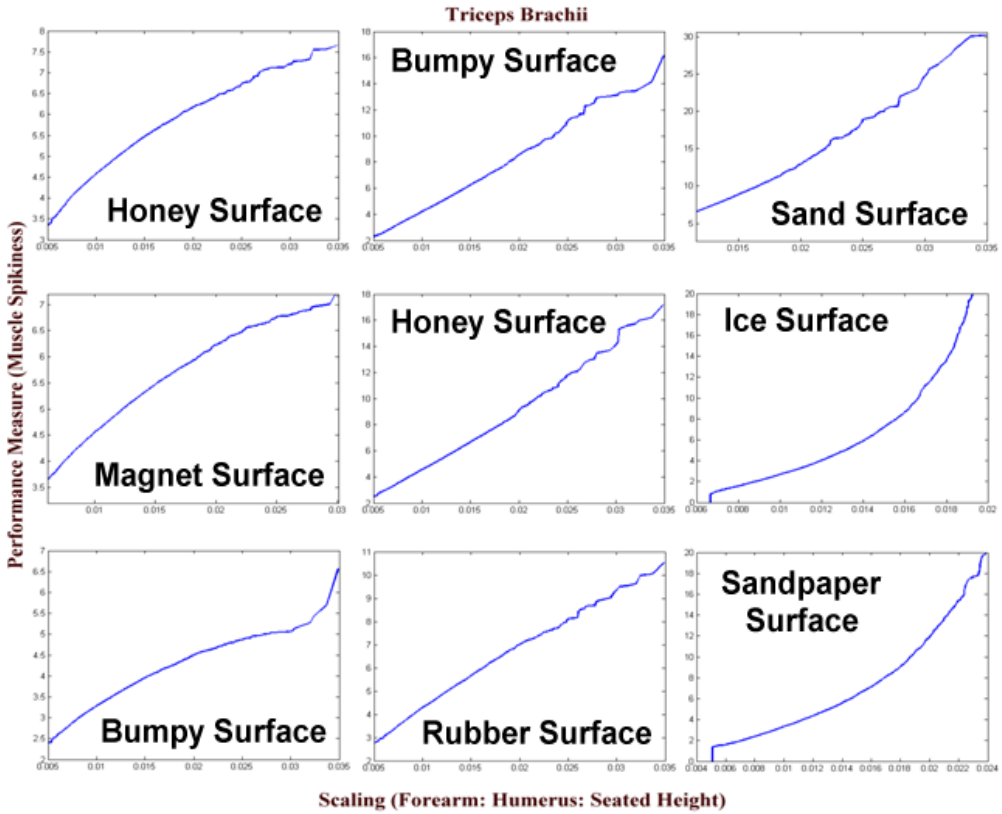

Figure 5. Results for the Monte Carlo simulations for the Triceps Brachii muscle and performance scaling (Forearm: Humerus: Seated Height).

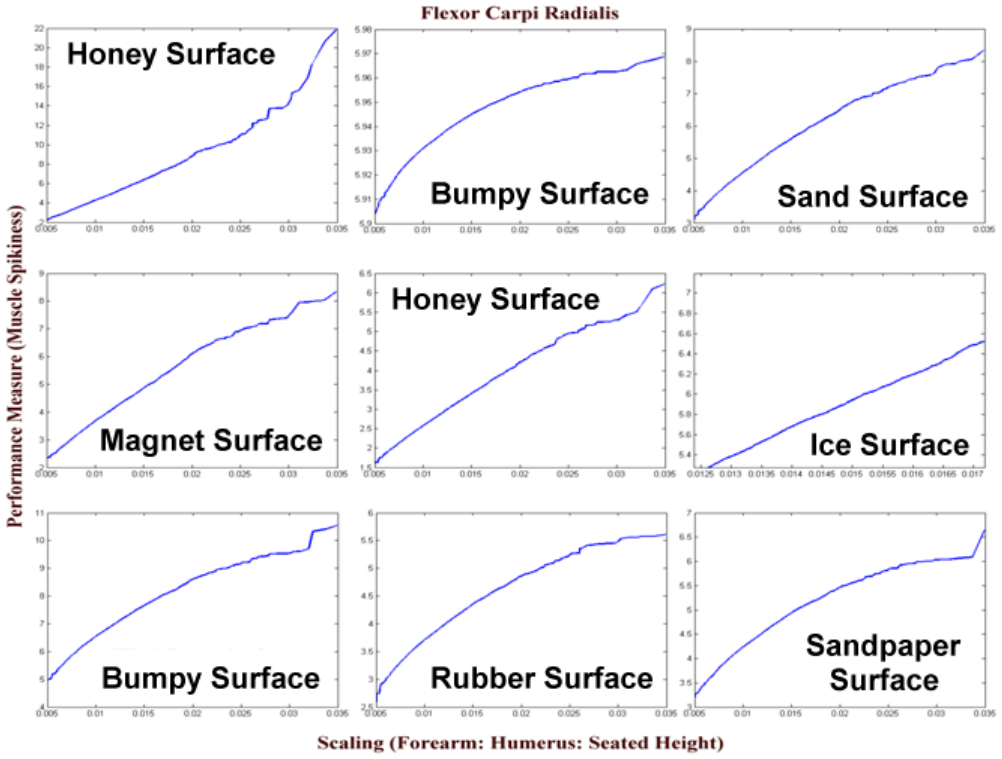

Figure 6. Results for the Monte Carlo simulations for the Flexor Carpi Radialis muscle and performance scaling (Forearm: Humerus: Seated Height).

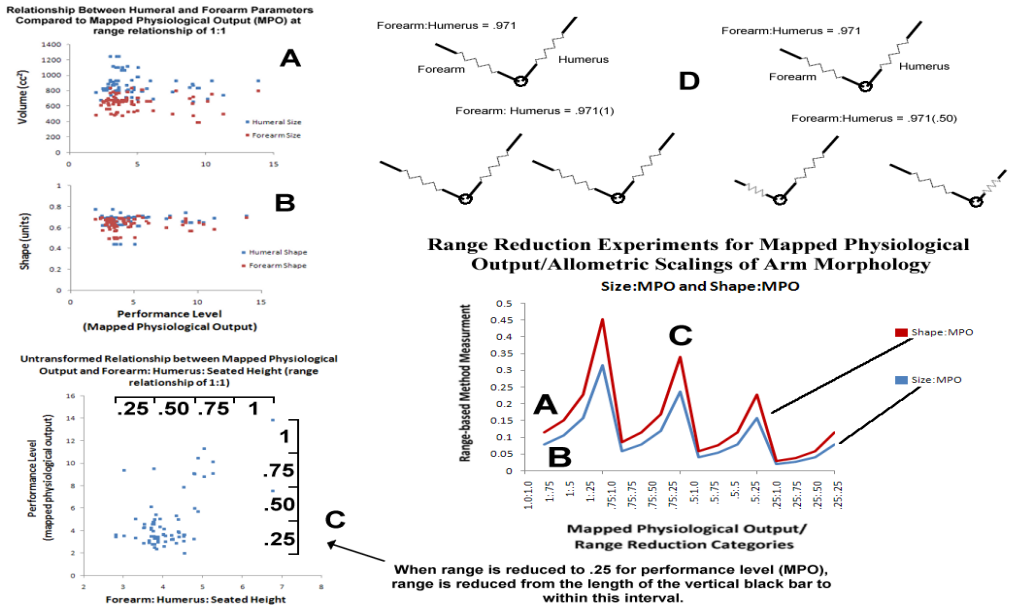

Figure 7. Results for range reduction experiments conducted on mapped physiological output data (range-based measurement averaged across experimental blocks) for Experiment #3. Main graph is displayed on right-hand side. Reduction categories are listed as *m,n*, where *m* is reduction/enlargement of performance measure, and n is reduction/enlargement of the allometric scaling. A and B represent the normal range of size and shape vs. performance level before range reduction. C is the relationship between performance scaling and performance level before range reduction. D is a biomechanical model of relationships between the scaling factor and the effect it would have on the arm.

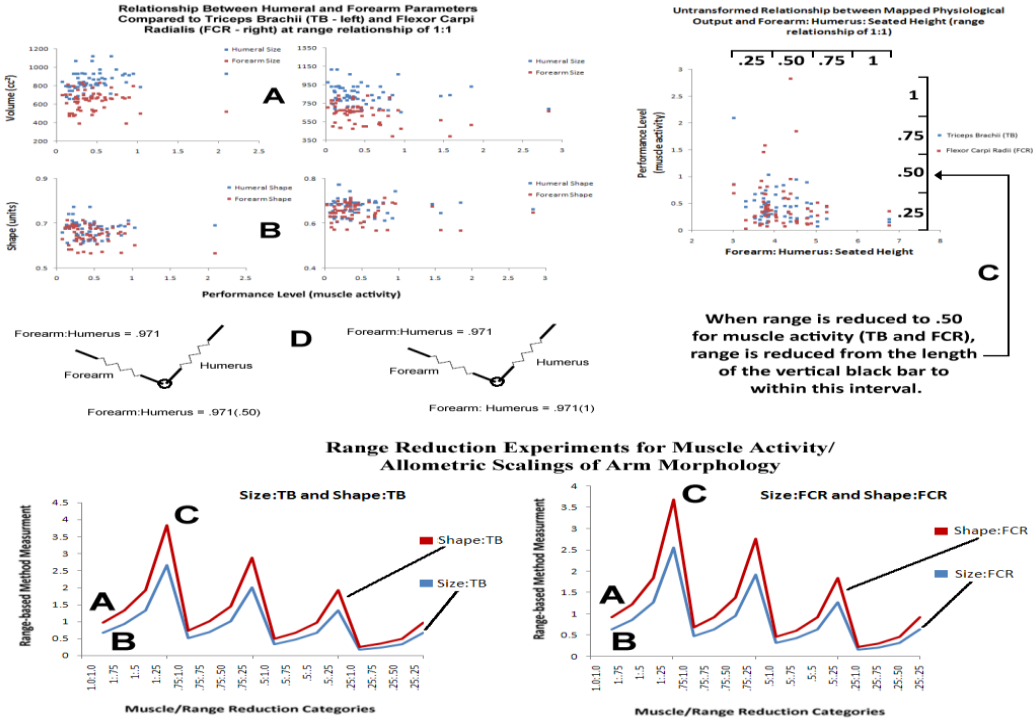

Figure 8. Results for range reduction experiments conducted on muscle activity data for Experiment #3. TB = triceps brachii, FCR = flexor carpi radialis (range-based measurement Figure averaged across experimental blocks). Main graph is displayed at bottom. Reduction categories are listed as *m,n*, where *m* is reduction/enlargement of performance measure, and n is reduction/enlargement of the allometric scaling. A and B represent the normal range of size and shape vs. performance level before range reduction. C is the relationship between performance scaling and performance level before range reduction. D is a biomechanical model of relationships between the scaling factor and the effect it would have on the arm.

Conclusions

The definition of a range-based technique is a way to simulate and model myriad changes in phenotype that result from biological and technological manipulation. There are at least three ways to get at this: rescale data based on limb geometry and performance measures by a series of percentages, finding an optimal point for the confluence of morphological size and performance indicators, and simulating existing morphological performance relationships to look for changes under a number of environmental conditions.

The demonstration presented in this paper is limited to neuromechanical systems. However, this general approach can be extrapolated to other problem domains. For example, other scaling laws such as the relationship between metabolic rate and body size may be better understood using this method. Moreover, this method may lead to principles that govern biological structure and organismal-environment interaction.

Table 2. Parameters for optimal relationships between performance and morphology[6].

MPO	**Median for Bin of Highest Density, Entropy of all bins (H)**	**F:H SIZE** (Median, H)	**F:H SHAPE** (Median, H)	**W:BS** (Median, H)
Interleaved	3.52, 0.50	0.69/0.86, 0.77	0.99/1.19, 0.89	0.78/0.82, 0.85
Early	3.52, 0.64	0.69/0.86, 0.77	0.99/1.19, 0.89	0.78/0.82, 0.85
Late	2.58, 0.71	0.69/0.86, 0.77	0.99/1.19, 0.89	0.78/0.82, 0.85
Control	3.52, 0.55	0.69/0.86, 0.77	0.99/1.19, 0.89	0.78/0.82, 0.85
TB				
Interleaved	0.21/1.72, 0.82	0.69/0.86, 0.77	0.99/1.19, 0.89	0.78/0.82, 0.85
Early	0.23/0.53, 0.77	0.69/0.86, 0.77	0.99/1.19, 0.89	0.78/0.82, 0.85
Late	0.21/1.17, 0.77	0.69/0.86, 0.77	0.99/1.19, 0.89	0.78/0.82, 0.85
Control	0.40, 0.97	0.69/0.86, 0.77	0.99/1.19, 0.89	0.78/0.82, 0.85
FCR				
Interleaved	1.04/1.55, 0.84	0.69/0.86, 0.77	0.99/1.19, 0.89	0.78/0.82, 0.85
Early	1.33/1.64, 0.90	0.69/0.86, 0.77	0.99/1.19, 0.89	0.78/0.82, 0.85
Late	0.67/1.37/2.06/3.1, 0.89	0.69/0.86, 0.77	0.99/1.19, 0.89	0.78/0.82, 0.85
Control	1.25/1.84, 0.79	0.69/0.86, 0.77	0.99/1.19, 0.89	0.78/0.82, 0.85
UMP-TB				
Interleaved	0.45, 0.09	0.69/0.86, 0.77	0.99/1.19, 0.89	0.78/0.82, 0.85
Early	0.35, 0.08	0.69/0.86, 0.77	0.99/1.19, 0.89	0.78/0.82, 0.85
Late	0.20, 0.10	0.69/0.86, 0.77	0.99/1.19, 0.89	0.78/0.82, 0.85
Control	0.42, 0.09	0.69/0.86, 0.77	0.99/1.19, 0.89	0.78/0.82, 0.85
UMP-FCR				
Interleaved	0.44, 0.16	0.69/0.86, 0.77	0.99/1.19, 0.89	0.78/0.82, 0.85
Early	0.44, 0.20	0.69/0.86, 0.77	0.99/1.19, 0.89	0.78/0.82, 0.85
Late	0.38, 0.24	0.69/0.86, 0.77	0.99/1.19, 0.89	0.78/0.82, 0.85
Control	0.41, 0.10	0.69/0.86, 0.77	0.99/1.19, 0.89	0.78/0.82, 0.85

[6] x.xx/x.xx represents a bimodal distribution (each number represents a peak in the distribution). Each peak is defined as a density .05 greater than any other point. For multiple peaks, the bins defined as peaks can be with .05 units of density, but all peaks follow the same definition.

Role of regulatory mechanisms in producing observed effects. One insight these approaches provide are the relative contributions of morphological control, neural control, and muscular control to adaptive responses. Certain features of morphology conform to the demands of performance across a range of conditions. In addition to understanding the contribution of each type of control, different regulatory mechanisms can be associated with the various types of control. For example, neural control is driven by an internal model which produces a ratchet-like mechanism for adaptation. In this case, a perturbation provides the means to explore a range of responses which loosely correspond to the physiological range of the individual. After this initial perturbation, the system finally settles into a stable state which will differ from the initial condition, but not as much as the response during the perturbation. Changes driven by muscular control may involve a robustness mechanism which provides a mechanism for adaptation that is semi-independent of the perturbation. Muscle fiber recruitment and protein expression in the cross bridges of the muscle fibers during contraction may allow for this robustness mechanism to compensate for morphological control and override neural control under certain conditions (Rome et al, 1999).

Methods and Measurements

Physiological Activity

To collect electrical potentials from the nervous system and information about internal physiological states, the Biopac MP150 biopotential amplification system was used (Biopac Systems, Goleta, CA). Two channels was used to collect these data from the muscles of the forearm and humerus.

A template was created in AcqKnowledge® (Biopac Systems, Goleta, CA) to digitize, smooth, and transform the raw data in real time. A sampling rate of 1000Hz was used to collect the raw data. A calculation channel with a window of 10 data points was used to smooth the muscle activity data using a moving average routine which resulted in a final sampling rate of 100 data points per second. A special calculation channel was used to apply an integrated EMG (iEMG) filter to rectify and mathematically integrate the signal representing muscle activity. The hardware filters were set to a gain of 5000, a high-pass analog filter value of 1Hz, and provided notch filtering of the signal (50dB rejection mode at 50-60Hz). A notch filter was used to remove ambient spectral noise.

Muscle activity

Electromyography (EMG)[7] was collected using the Biopac MP150 system (Biopac Systems, Goleta, CA) to quantify muscle activity. Multiple segments act semi-independently to determine the consequences of sensory input, feedback, and variability. Two points on the upper arm were selected to record EMG data: the flexor carpi radialis[8] along the forearm and the triceps brachii[9] along the humerus. Muscle activity at these locations can be used to determine arm movements in relation to dynamic upper-body posture (see Figure 9).

The muscles recorded in these experiments were selected based on two factors: muscles that were located along the dorsal or ventral surface of the arm, and muscles that were involved in the complex reaching movement. Several steps were taken to ensure the internal validity of these measurements[10].

---

[7] Electromyography (EMG) is a method of recording electrical activity from specific muscles to quantify changes in firing relative to anatomical movement. The power of an EMG signal is roughly equivalent to action potentials fired in response to reflexive behavior or anticipatory single sent from the sensorimotor brain centers.

[8] A muscle of the forearm that acts to flex (contract) and abduct the hand. Flexor carpi radialis inserts proximally at the medial epicondyle of the humerus and distally at the base of the fifth metacarpal.

[9] A muscle of the humerus involved in extension. Triceps brachii helps to keep the arm straightened in the face of resistance, and inserts distally at the olecranon process of the ulna.

[10] The muscles were located using a digital musculoskeletal atlas (http://rad.washington.edu/atlas), measurements of the arm's surface, and palpatation. These locations were confirmed by testing the preparation before recording. The trace recording was assessed for muscle spindle activity and ECG artifact during one instance of complex reaching. If any abnormalities were detected, the preparation was redone along with relocation of the surface electrodes. The connections were checked with an impedance meter before the experiment began and periodically in between blocks.

Mapped Physiological Output Measurement

A measurement of mapped physiological output was calculated for several reaches over the course of a two-minute trial. This is a measure original to this document. While it is not a direct measure of force, it is related to how afferent signals from the nervous system are attenuated while virtual objects are being controlled in a virtual environment. Mapped physiological output was measured using the following equation

$$\mathbf{MPO}_t = |\mathbf{D}_{req} + \mathbf{D}_{moved}| \quad [1]$$

where D_{req} is the fixed distance a virtual object needs to be moved over a given trial, D_{moved} is the distance the virtual object is actually moved resulting from muscle force production captured by the input device, and MPO_t is the mapped physiological output for a single reach using the prosthetic device. A single reach will consist of taking a swing with the prosthetic interface. The operator will start each swing aligned with markers on the floor that denote a baseline or resting physical state. The distance the ball travels in the simulation and a completion time constant was collected. For each reach, the simulation was reset so that the shot is always taken from the beginning of the first hole. Sixteen reaches were administered across a single experimental block.

Phenotypic assays

Phenotypic assays were collected for each participant prior to the experimental session (see Figure 9). The following measurements were taken: forearm, humerus, lower body height, and total height. All measurements are taken prior to being seated at the interface. A measuring tape was used to collect all measurements listed herein. The measurements listed in this section are the measurements that were directly measured from the participant. The following measurements were calculated from the empirical data: total arm length (AL), humerus length (H), head and trunk (HAT) height, shank length (SL), and thigh length (TL).

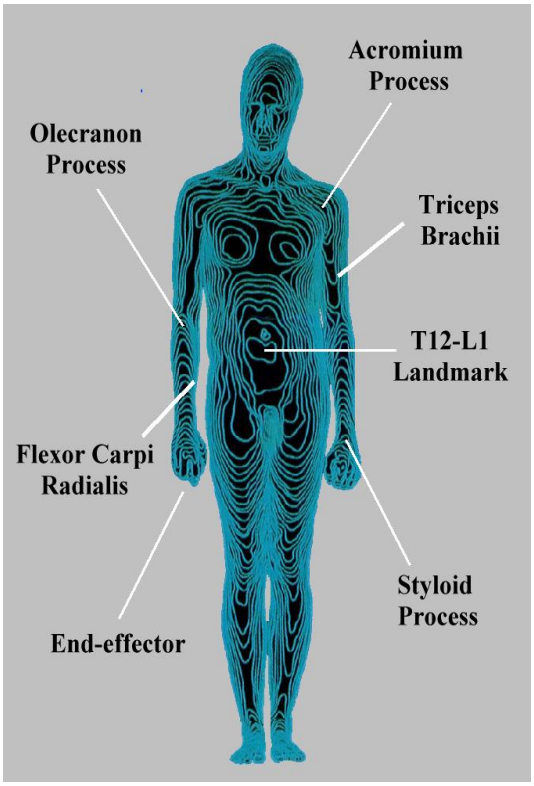

Figure 9. Configuration of the major anatomical landmarks, muscles, and interaction points explored in this document.

The total height measurements involve subjects standing in an upright posture with their backs against the wall. A yardstick was affixed to the wall immediately behind the subject. The total height (TH) measurement was taken from the feet to the saggital crest at the top of the head. This measurement was measured before the experiment and used as a constant in calculating the HAT measurement. For measurements of the arms and upper body, subjects will remain standing but away from the wall. The method of Martin and Nguyen (2004) was used to assay arm length and biacromial breadth,

head and trunk (see Winter, 1990, Chapter 4), and lower body measurements. Participants will extend their arms, hands, and fingers maximally outward from their sides so that the subject's wingspan can be measured.

Using this pose, the experimenter obtained four upper-body measurements. The first is shoulder breadth, defined as the distance from the left acromioclavicular (AC) joint to the right AC joint. The second is total wingspan, defined here as the distance from the left styloid process (distal end of the ulna) to the right styloid process (distal end of the ulna). The third measurement is forearm length, which was taken on both the right and left arms from the elbow joint (olecranon process - proximal end of forearm segment) to the styloid process (distal end of the ulna – distal end). The fourth measurement is humerus length, which was taken on both the right and left arms from the olecranon process (elbow joint) to the AC joint.

Measurements should be straight-line, one-dimensional assays along the dorsal surface of the coronal plane. The total arm and humerus lengths can be derived from these measurements. Total arm length (AL) can be calculated by the following equation

$$\mathbf{AL = (TWS - BB) / 2} \qquad \mathbf{[2]}$$

where TWS is the total wingspan and BB is the bicromial breadth. Humerus length (H) can be calculated as

$$\mathbf{H = AL - F} \qquad \mathbf{[3]}$$

where AL is the arm length and F is the forearm length.

Constructs and Conceptual Measurement

Performance level. Performance level serves as a dependent variable. A decrease in mean EMG spectral power and decreased behavioral variability during each block of an experimental condition as reflected in mapped physiological output can often be considered different dimensions of improved performance. Generally, performance level can be defined using the following equation

$$\mathbf{L_p = \sum PM_t / t} \qquad \mathbf{[4]}$$

where L_p is the level of performance, PM is the performance measurement, and t is the number of trials being averaged. The performance measurement represents either the mapped physiological output calculation or aggregate spectral transformations of the physiological recordings. These are complementary measures of performance improvement or degradation given the current environmental state or experimental phase. When performance level is compared across experimental phases, as in the case with decreased EMG activity, it is also a measure of adaptation.

Inertial Feedback. A concept related to unlearning is called inertial feedback. Mechanical sensory information provided by movement generated against an environmental medium can best be conceptualized as a volume of information that envelops the individual and acts as a "medium" enveloping the operator (see Snyder et.al, 2007 for application). Turbulence caused by force generated against this medium may play a key role in augmenting the function of sensorimotor integration mechanisms in the central nervous system (Nishikawa et.al, 2007). In the case of organisms that are entirely immersed in a specific environmental medium such as water, this information is quantified by the Reynolds number (Bejan and Marden, 2006), which approximates the viscosity and resistance of the body morphology to the environment as it acts against the body. To approximate the characteristics of this fluidity and resistance for the upper limbs in the context of mutating the environment, a forcing chamber on a prosthetic device was used. The inertial effects of the forcing chamber were kept constant by filling it with water at room temperature. This medium has a specific density of 1, which can be defined as

$$\mathbf{d_S = W / vol} \qquad \mathbf{[5]}$$

where d_S is specific density, W is the weight, and vol is the volume.

Bounds of Adaptability. The bounds of adaptability serve as an independent variable. The degradation of visual inputs in the experimental phases using the naked controller and limb lengths serve as boundaries to functional performance. One way the bounds of adaptability can be quantified is by mathematically scaling two or more phenotypic assays. One example of this is the scaling of total height to forearm length. This scaling is called static allometry, which when used as a predictor of performance level can be defined as

$$\mathbf{Y = -Ax^2 + Bx - c} \qquad \mathbf{[6]}$$

where Y describes a second-order polynomial. This particular definition of functional static allometry, which characterizes specific body sizes and shapes attained at the end of development, is based on growth regulation in development and may have an optimizing effect on performance (Garcia and Leal da Silva, 2006; Herr et.al, 2002). This variable serves as an aspect of the phenotype for specific experimental conditions.

Notes on experimental procedures

Three different experiments were conducted to derived data used in this paper. Two of them involved reaching to hit a target over the course of a single trial. Using a motion-based virtual environment, movement using a motion controller and a weighted rod was interspersed with movement using the motion controller only. The first of these experiments utilized three experimental blocks consisting of 16 trials apiece. The other one of these experiments utilized five blocks consisting of 16 trials apiece. Perturbation in these experiments was defined as movement over the course of a block using a device of one type (either weighted rod or no weighted rod) delivered either as the first block in the experiment or in between blocks featuring the opposite treatment type. In the first experiment of this type, four conditions were introduced in a between-subjects manner: 1) weighted rod, no weighted rod, weighted rod, 2) no weighted rod, weighted rod, no weighted rod, 3) weighted rod, no weighted rod, no weighted rod, and 4) no weighted rod, weighted rod, weighted rod. In the other experiment of this type, four conditions were introduced in a between-subjects manner: 1) no weighted rod, weighted rod, no weighted rod, weighted rod, no weighted rod, 2) weighted rod, weighted rod, no weighted rod, no weighted rod, no weighted rod, 3) no weighted rod, no weighted rod, weighted rod, weighted rod, weighted rod, and 4) no weighted rod, no weighted rod, no weighted rod, no weighted rod, no weighted rod. The experiment from which the Monte Carlo simulation was derived involved a force-feedback device and virtual environment presentation of different tactile stimuli. Each block (three total) involved a three-minute bout of free exploration. To induce a perturbation in this experiment, surfaces of the same type (hard or soft) were interspersed between blocks featuring surfaces of the opposite type. Three conditions were introduce in a between-subjects manner: 1) magnet, honey, and ice, 2) bumpy, rubber, and sandpaper, and 3) honey, bumpy, and sand.

References:

Alicea, B. Performance Augmentation in Hybrid Systems: techniques and experiment. arXiv Repository, arXiv:0810.4629 [q-bio.NC, cs.HC] (2008).

Barry, B.K. and Enoka, R.M. The neurobiology of muscle fatigue: 15 years later. Integrative and Comparative Biology, 47(4), 465-473 (2007).

Bejan, A. and Marden, J.H. Unifying constructal theory for scale effects in running, swimming, and flying. Journal of Experimental Biology, 209, 238-248 (2006).

Bejan, A. Shape and Structure: from engineering to nature. Cambridge University Press, Cambridge, MA (2000).

Brown, J.H., Enquist, B.J., and West, G.B. The fourth dimension of life: fractal geometry and allometric scaling of organisms. Science, 284, 1677-1678 (1999).

Brown, J. H., Enquist, B. J. & West, G. B. A general model for the origin of allometric scaling laws in biology. Science, 276, 122-126 (1997).

Cheverud, J.M. Relationships among ontogenetic, static, and evolutionary allometry. American Journal of Physical Anthropology, 59, 139-149 (1982).

Collins, S., Ruina, A., Tedrake, R., and Wisse, M. Efficient bipedal robots based on passive-dynamic walkers. Science, 307, 1082-1085 (2005).

Emlen, D.J. and Allen, C.E. Genotype to Phenotype: Physiological Control of Trait Size and Scaling in Insects. Integrative and Comparative Biology, 43, 617–634 (2004).

Enoka, R. Neuromechanics of Human Movement. Human Kinetics, Champaign, IL (2002).

Full, R. J. and Koditschek, D. E. Templates and anchors: neuromechanical hypotheses of legged locomotion on land.

Journal of Experimental Biology, 202, 3325–3332 (1999).

Garcia, G.J.M. and Leal da Silva, J.K. Interspecific allometry of bone dimensions: A review of the theoretical models. Physics of Life Reviews, 3(3), 188-209 (2006).

Gomi, H. and Kawato, M. Equilibrium-point control hypothesis examined by measured arm stiffness during multijoint movement. Science, 272(5258), 117-120 (1996).

Hara, F. and Pfeifer, R. Morpho-Functional Machines: The New Species: Designing Embodied Intelligence. Springer, Berlin (2003).

Herr, H.M., Huang, G.T., and McMahon, T.A. A model of scale effects in mammalian quadrupedal running. Journal of Experimental Biology, 205, 959-967 (2002).

Holmes, P., Full, R.J., Koditschek, D., Guckenheimer, J. The Dynamics of Legged Locomotion: Models, Analyses, and Challenges. SIAM Review, 48(2), 207-304 (2006).

Hurst, H.E. Long-term storage-capacity of reservoirs. Transactions of the American Society of Civil Engineering, 116, 770-808 (1951).

Huxley, J.S. Problems of relative growth. Dial Press, New York (1932).

Martin, J.T. and Nguyen, D.H. Anthropometric analysis of homosexuals and heterosexuals: implications for early hormone exposure. Hormones and Behavior, 45, 31–39 (2004).

Nishikawa, K., Biewener, A.A., Aerts, P., Ahn, A.N., Chiel, H.J., Daley, M.A., Daniel, T.L., Full, R.J., Hale, M.E., Hedrick, T.L., Lappin, A.K., Nichols, T.R., Quinn, R.D., Satterlie, R.A., and Szymik, B. Neuromechanics: an integrative approach for understanding motor control. Integrative and Comparative Biology, 47(1), 16-54 (2007).

Rome, L.C., Cook, C., Syme, D., Connaughton, M., Ashley-Ross, M., Klimov, A., Tikunov, B. and Goldman, Y.E. Trading force for speed: crossbridge kinetics of super-fast muscle fibers. PNAS USA, 96, 5826-5831 (1999).

Scholz, J.P. and Schoner, G. The uncontrolled manifold concept: identifying control variables for a functional task. Experimental Brain Research, 126(3), 289-306 (1999).

Snyder, J.B., Nelson, M.E., Burdick, J.W., MacIver, M.A. Omnidirectional sensory and motor volumes in electric fish. PLoS Biology, 5(11), e301 (2007).

West, G.B. and Brown, J.H. The origin of allometric scaling laws in biology from genomes to ecosystems: towards a quantitative unifying theory of biological structure and organization. The Journal of Experimental Biology, 208, 1575-1592 (2005).

West, G.B., Brown, J.H, Enquist, B.J. A General Model for the Origin of Allometric Scaling Laws in Biology. Science, 276, 122-126 (1997).

Winter, D.A. Biomechanics and Motor Control of Human Movement. Wiley, New York (1990).